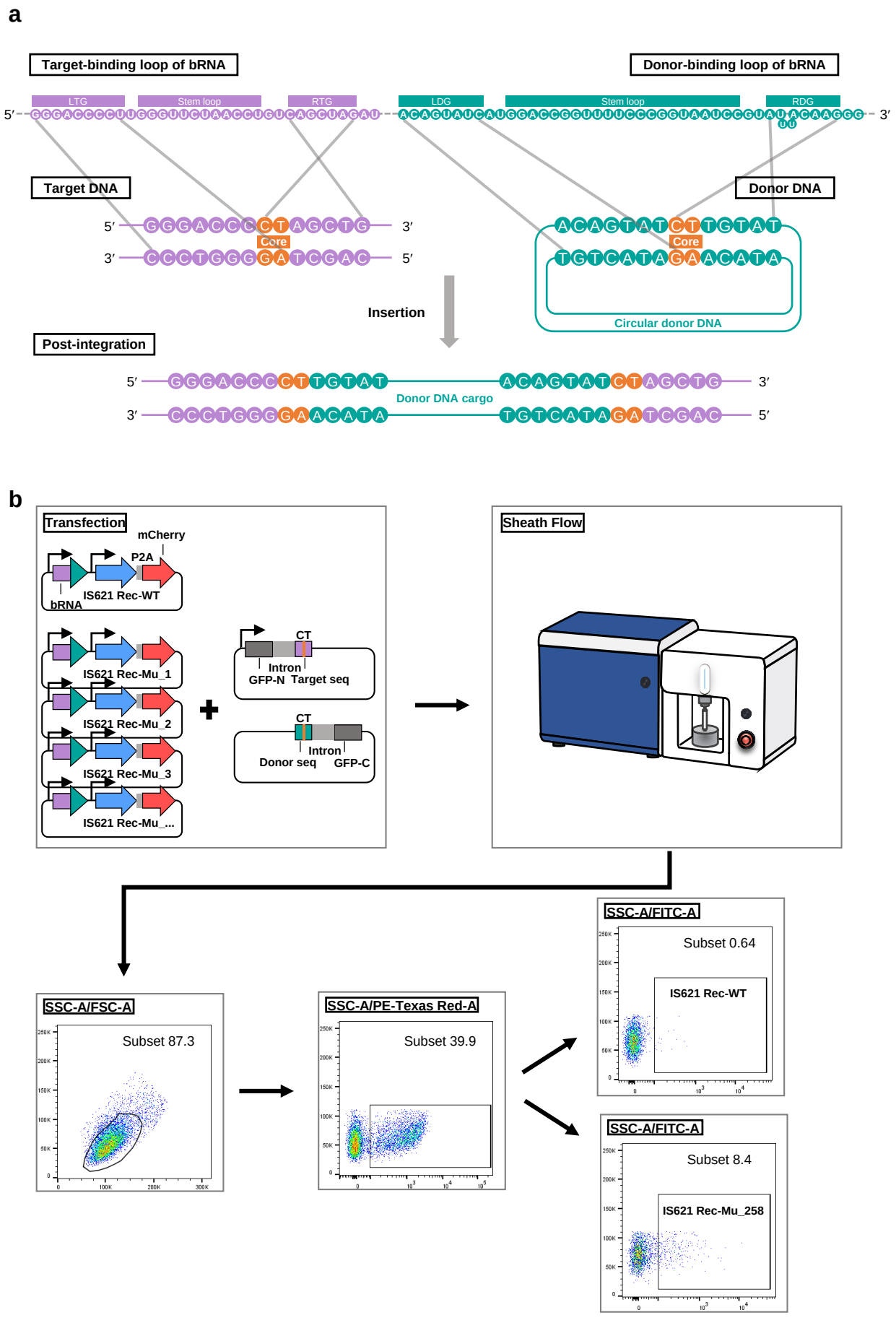
a
Target-binding loop of bRNA
Donor-binding loop of bRNA
LTG
Stem loop
RTG
LDG
Stem loop
RDG
5′
3′
Target DNA
Donor DNA
Core
Core
Insertion
Post-integration
Donor DNA cargo
Circular donor DNA
b
Transfection
mCherry
P2A
bRNA
IS621 Rec-WT
IS621 Rec-Mu_1
IS621 Rec-Mu_2
IS621 Rec-Mu_3
IS621 Rec-Mu_...
CT
Intron
GFP-N Target seq
CT
Intron
Donor seq
GFP-C
Sheath Flow
SSC-A/FSC-A
Subset 87.3
SSC-A/PE-Texas Red-A
Subset 39.9
SSC-A/FITC-A
Subset 0.64
IS621 Rec-WT
SSC-A/FITC-A
Subset 8.4
IS621 Rec-Mu_258

Supplementary Figure 1:Schematic overview of IS621 recombinase–mediated DNA insertion and flow cytometry gating strategy used for IS621-bRNA engineering.
a, Schematic illustration of base-pairing interactions between the bRNA and tDNA or dDNA, and the resulting DNA insertion mediated by the IS621 recombinase. The bRNA is shown on top in a linear form. The regions corresponding to the target-binding loop (TBL) and donor-binding loop (DBL) are marked in purple and green, respectively. The target DNA and the donor DNA are shown schematically underneath the bRNA, where the CT cores are marked in orange. The base pairing between regions of TBL and DBL with the DNAs are delineated by grey lines. Note that as the 3′ portion of TBL and of DBL respectively form a “reverse” side of the binding loops, their pairing with the top strand of target and donor DNA is marked by lines in a crossed fashion. **b,** Flow cytometry analysis of insertion efficiency following engineering of the IS621-bRNA system. The main cell population was identified based on FSC-A and SSC-A. Transfected cells were subsequently gated using PE–Texas Red-A fluorescence, and DNA insertion efficiency mediated by the engineered IS621-bRNA system was quantified based on FITC-A fluorescence intensity.

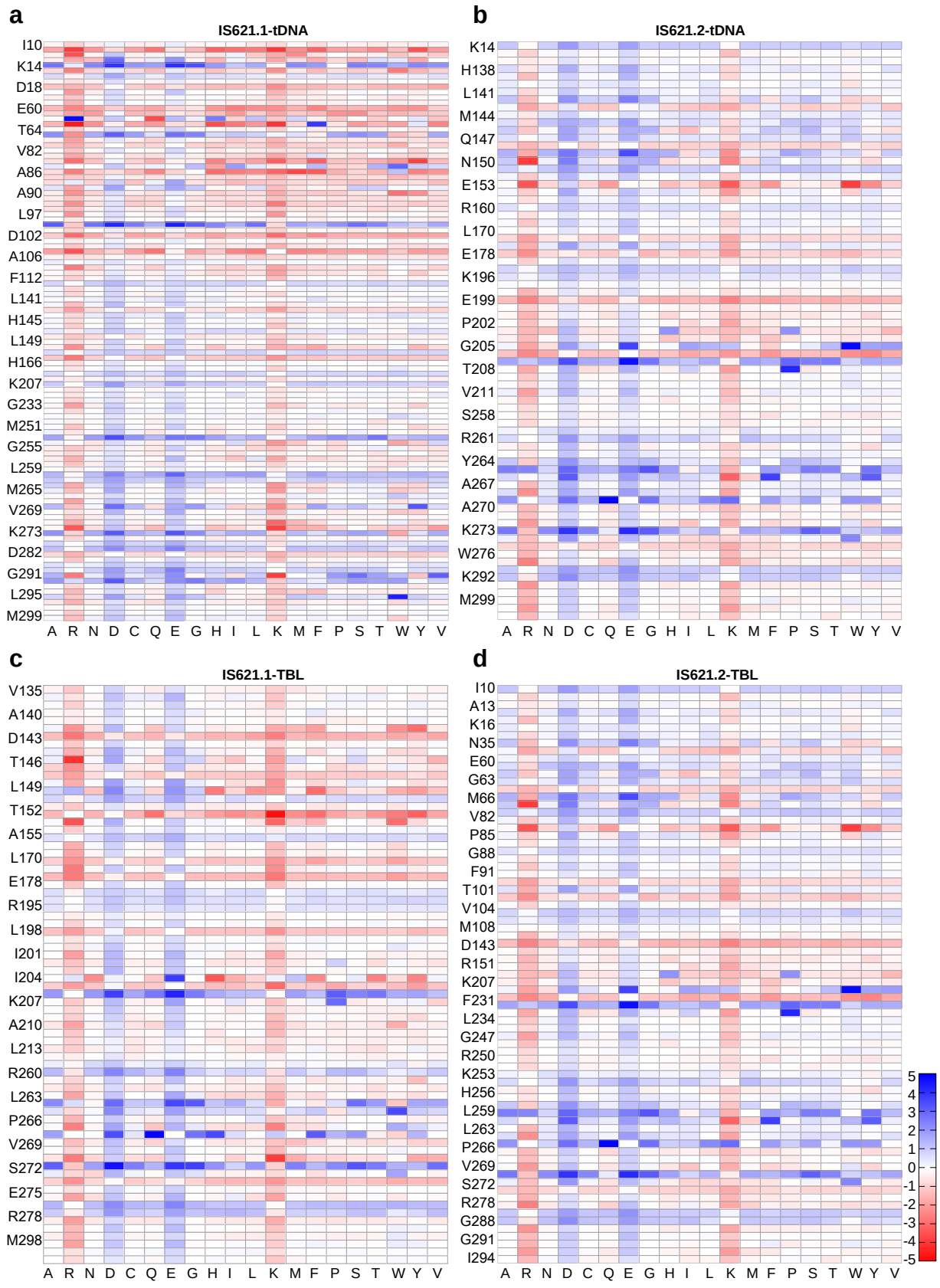
a
IS621.1-tDNA
I10
K14
D18
E60
T64
V82
A86
A90
L97
D102
A106
F112
L141
H145
L149
H166
K207
G233
M251
G255
L259
M265
V269
K273
D282
G291
L295
M299
A R N D C Q E G H I L K M F P S T W Y V
b
IS621.2-tDNA
K14
H138
L141
M144
Q147
N150
E153
R160
L170
E178
K196
E199
P202
G205
T208
V211
S258
R261
Y264
A267
A270
K273
W276
K292
M299
A R N D C Q E G H I L K M F P S T W Y V
c
IS621.1-TBL
V135
A140
D143
T146
L149
T152
A155
L170
E178
R195
L198
I201
I204
K207
A210
L213
R260
L263
P266
V269
S272
E275
R278
M298
A R N D C Q E G H I L K M F P S T W Y V
d
IS621.2-TBL
I10
A13
K16
N35
E60
G63
M66
V82
P85
G88
F91
T101
V104
M108
D143
R151
K207
F231
L234
G247
R250
K253
H256
L259
L263
P266
V269
S272
R278
G288
G291
I294
A R N D C Q E G H I L K M F P S T W Y V
5
4
3
2
1
0
-1
-2
-3
-4
-5

Supplementary Figure 2: Binding affinity landscape of IS621 monomers for tDNA and TBL. **a-d,** The heat map shows the predicted binding affinities (kcal/mol) of IS621 to DNA or RNA at each amino acid position when substituted with the other 19 amino acids. As the PDB structure contains two IS621 monomers, binding affinity changes were calculated for each monomer independently. Results for the two monomers are presented separately for tDNA (**a, b**) and for TBL (**c, d**).

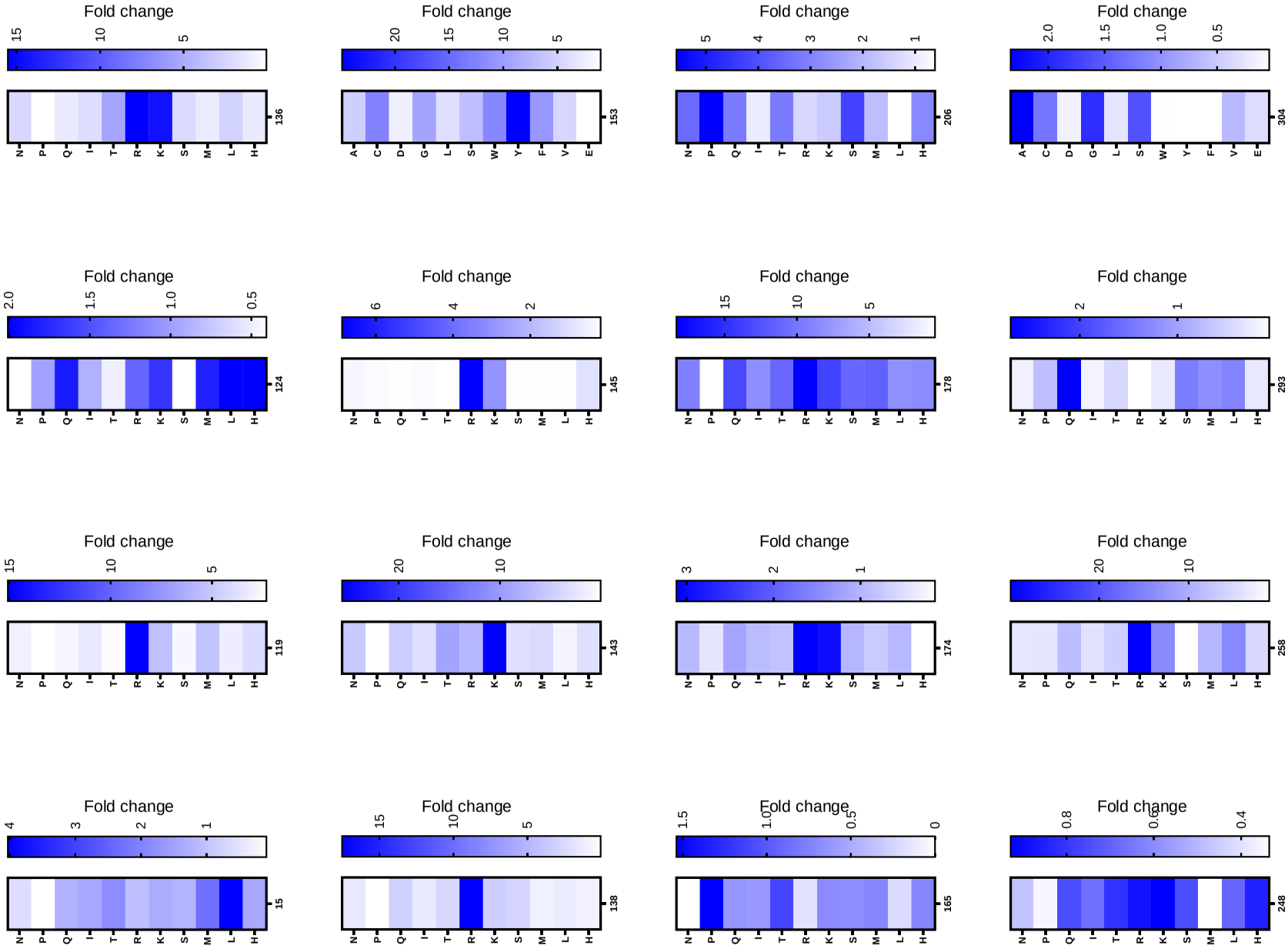
Fold change
15
10
5
N P Q I T R K S M L H
136
Fold change
20
15
10
5
A C D G L S W Y F V E
153
Fold change
5
4
3
2
1
N P Q I T R K S M L H
206
Fold change
2.0
1.5
1.0
0.5
A C D G L S W Y F V E
304
Fold change
2.0
1.5
1.0
0.5
N P Q I T R K S M L H
124
Fold change
6
4
2
N P Q I T R K S M L H
145
Fold change
15
10
5
N P Q I T R K S M L H
178
Fold change
2
1
N P Q I T R K S M L H
293
Fold change
15
10
5
N P Q I T R K S M L H
119
Fold change
20
10
N P Q I T R K S M L H
143
Fold change
3
2
1
N P Q I T R K S M L H
174
Fold change
20
10
N P Q I T R K S M L H
258
Fold change
4
3
2
1
N P Q I T R K S M L H
15
Fold change
15
10
5
N P Q I T R K S M L H
138
Fold change
1.5
1.0
0.5
0
N P Q I T R K S M L H
165
Fold change
0.8
0.6
0.4
N P Q I T R K S M L H
248

Supplementary Figure 3: Relative insertion efficiency of IS621 recombinase after single amino acid substitutions.
Positions that showed enhanced activity following substitution with KNB or MNB libraries were further resolved into individual amino acid types to identify the most effective substitution at each position, related to Fig. 1c. All data are presented as means $\pm$ s.d. $n = 3$ independent biological replicates.

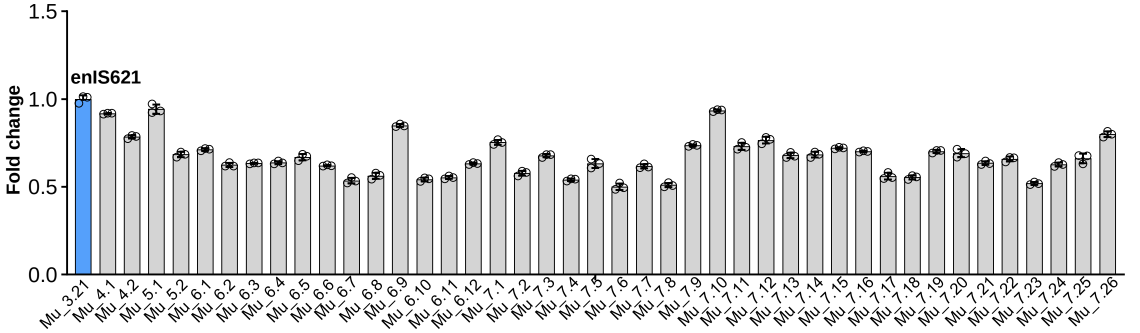

	Mu_3.21	Mu_4.1	Mu_4.2	Mu_5.1	Mu_5.2	Mu_6.1	Mu_6.2	Mu_6.3	Mu_6.4	Mu_6.5	Mu_6.6	Mu_6.7	Mu_6.8	Mu_6.9	Mu_6.10	Mu_6.11	Mu_6.12	Mu_7.1	Mu_7.2	Mu_7.3	Mu_7.4	Mu_7.5	Mu_7.6	Mu_7.7	Mu_7.8	Mu_7.9	Mu_7.10	Mu_7.11	Mu_7.12	Mu_7.13	Mu_7.14	Mu_7.15	Mu_7.16	Mu_7.17	Mu_7.18	Mu_7.19	Mu_7.20	Mu_7.21	Mu_7.22	Mu_7.23	Mu_7.24	Mu_7.25	Mu_7.26
E15L	-	-	-	-	-	-	-	-	-	-	-	-	-	-	-	-	-	-	-	-	-	-	-	-	-	-	-	-	-	-	-	-	-	-	-	-	-	-	-	-	-	-	-
A119R	+	+	+	+	-	-	+	+	+	+	+	+	+	+	+	+	+	-	+	+	+	+	+	+	+	+	+	+	+	+	+	+	+	+	+	+	+	+	+	+	+	+	+
P124H	-	-	-	-	-	-	+	+	+	-	-	-	-	-	-	-	-	-	+	+	+	+	-	-	-	-	-	-	-	-	+	+	-	-	-	-	-	-	-	-	-	-	-
V136R	-	-	-	-	-	-	-	-	-	+	+	+	-	-	-	-	-	-	-	-	-	-	+	+	-	-	-	-	-	-	-	-	+	+	+	-	-	-	-	-	-	-	-
H138R	+	-	-	-	-	-	-	-	-	-	-	-	+	-	-	-	-	-	-	-	-	-	-	-	+	+	-	-	-	-	-	-	-	-	-	-	-	-	-	-	-	-	-
D143K	-	-	-	-	+	+	+	-	-	+	-	-	-	-	-	-	-	-	+	-	-	-	-	-	-	-	+	-	-	-	+		+	-	-	-	-	-	-	+	-	-	-
H145R	-	-	-	-	-	-	-	+	-	-	-	-	-	+	+	-	+	+	-	+	-	-	-	-	-	-	-	+	+	-	-	+	-	-	-	+	+	+	-	-	+	+	+
E153Y	-	+	+	+	+	+	+	+	+	+	+	+	+	+	+	+	+	+	+	+	+	+	+	+	+	+	+	+	+	+	+	+	+	+	+	+	+	+	+	+	+	+	-
A165P	-	-	-	-	-	-	-	-	+	-	+	-	+	+		+	+	+	-	-	+	-	+	+	+	+	+	+		+	-	-	-	+	-	+	-	-	+	-	+	-	+
L174K	-	-	-	-	+	+	-	-	-	-	-	+	-	-	+	-	-	+	-	-	-	+	-	-	-	-	-	-	+	+	-	-	-	-	+	-	+	-	+	+	-	+	+
E178R	-	-	-	-	-	-	-	-	-	-	-	-	-	-	-	+	-	-	-	-	-	-	-	-	-	-	-	-	-	-	-	-	-	-	-	-	-	+	-	-	-	-	-
E206P	-	+	-	+	+	+	+	+	+	+	+	+	+	+	+	+	-	+	+	+	+	+	+	+	+	+	+	+	+	+	+	+	+	+	+	+	+	+	+	-	-	-	-
S258R	-	-	+	+	-	+	-	-	-	-	-	-	-	-	-	-	+	+	+	+	+	+	+	+	+	+	+	+	+	+	-	-	-	-	-	-	-	-	-	+	+	+	+
V293Q	+	-	-	+	-	+	-	-	-	-	-	-	-	-	-	-	-	+	+	+	+	+	+	+	+	+	+	+	+	+	+	+	+	+	+	+	+	+	+	+	+	+	+
Q304A	-	+	+	-	+	-	+	+	+	+	+	+	+	+	+	+	+	-	-	-	-	-	-	-	-	-	-	-	-	-	+	+	+	+	+	+	+	+	+	+	+	+	+

Supplementary Figure 4: Relative insertion efficiency of IS621 mutant proteins containing multiple single amino acid substitutions compared with enIS621.
The multi-mutant variants include triple, quadruple, quintuple, sextuple, and septuple combinations. Blue bars indicate the normalized insertion efficiency of enIS621. All data are presented as means ± s.d. $n = 3$ independent biological replicates.

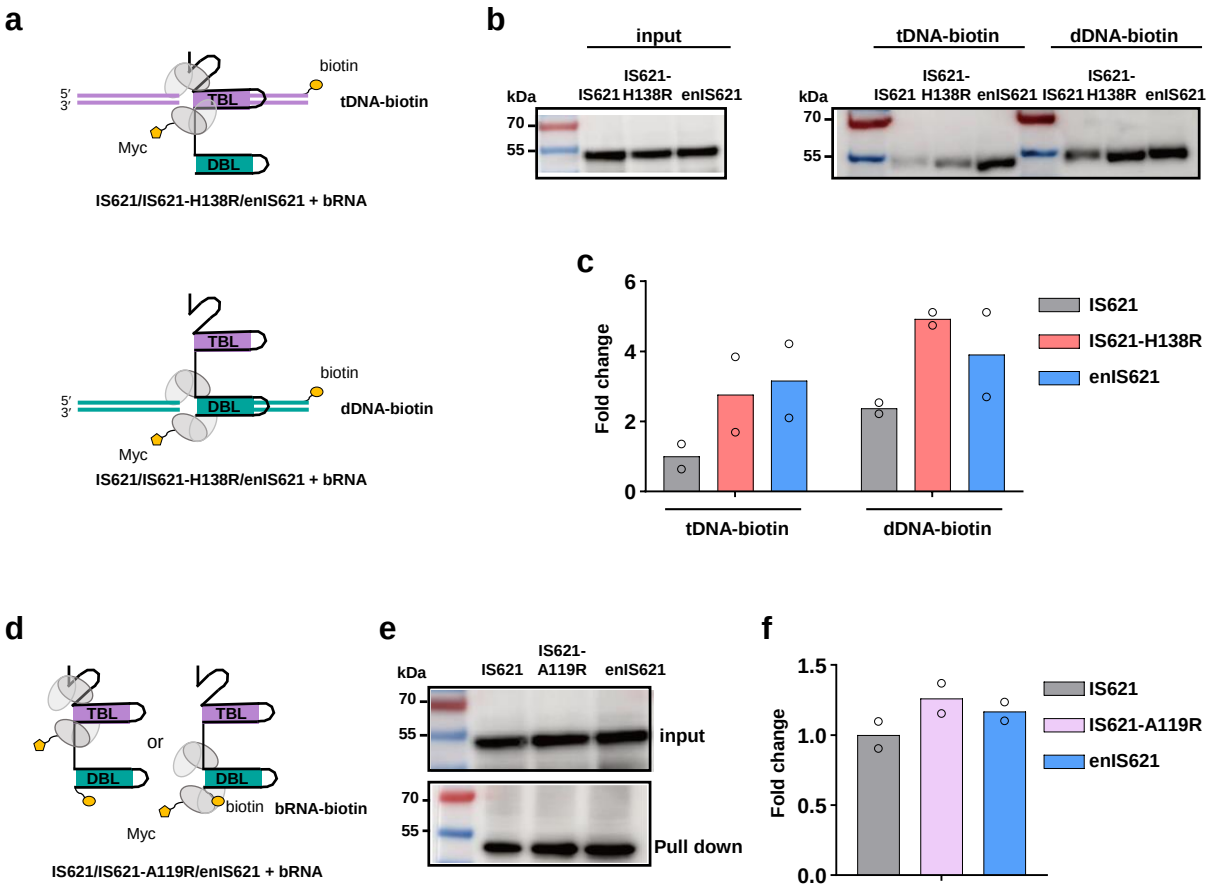
a
biotin
5′
3′
TBL
tDNA-biotin
Myc
DBL
IS621/IS621-H138R/enIS621 + bRNA
TBL
biotin
5′
3′
DBL
dDNA-biotin
Myc
IS621/IS621-H138R/enIS621 + bRNA
b
input
tDNA-biotin
dDNA-biotin
kDa
IS621
IS621-H138R
enIS621
70
55
c
Fold change
6
4
2
0
IS621
IS621-H138R
enIS621
tDNA-biotin
dDNA-biotin
d
TBL
TBL
or
DBL
DBL
biotin
bRNA-biotin
Myc
IS621/IS621-A119R/enIS621 + bRNA
e
kDa
IS621
IS621-A119R
enIS621
70
55
input
70
55
Pull down
f
Fold change
1.5
1.0
0.5
0.0
IS621
IS621-A119R
enIS621

Supplementary Figure 5: Mechanistic analysis of enhanced insertion editing efficiency mediated by the H138R, A119R, and V293Q mutations in enIS621 recombinase.
a, Schematic representation of pull-down assays using biotinylated 44-bp tDNA or 44-bp dDNA to capture IS621, IS621-H138R, and enIS621 proteins. **b,** Western blot analysis of IS621, IS621-H138R, and enIS621 proteins enriched by biotin-tDNA or biotin-dDNA pull-down assays. **c,** Quantification of fold changes in protein enrichment following biotin-tDNA or biotin-dDNA pull-down, normalized to wild-type IS621. **d,** Schematic representation of pull-down assays using biotinylated 177-nt bRNA to capture IS621, IS621-A119R, and enIS621 proteins. **e,** Western blot analysis of IS621, IS621-A119R, and enIS621 proteins enriched by biotin-bRNA pull-down assays. **f,** Quantification of fold changes in protein enrichment following biotin-bRNA pull-down, normalized to wild-type IS621. Data are presented as means ± s.d., $n = 2$ independent biological replicates.

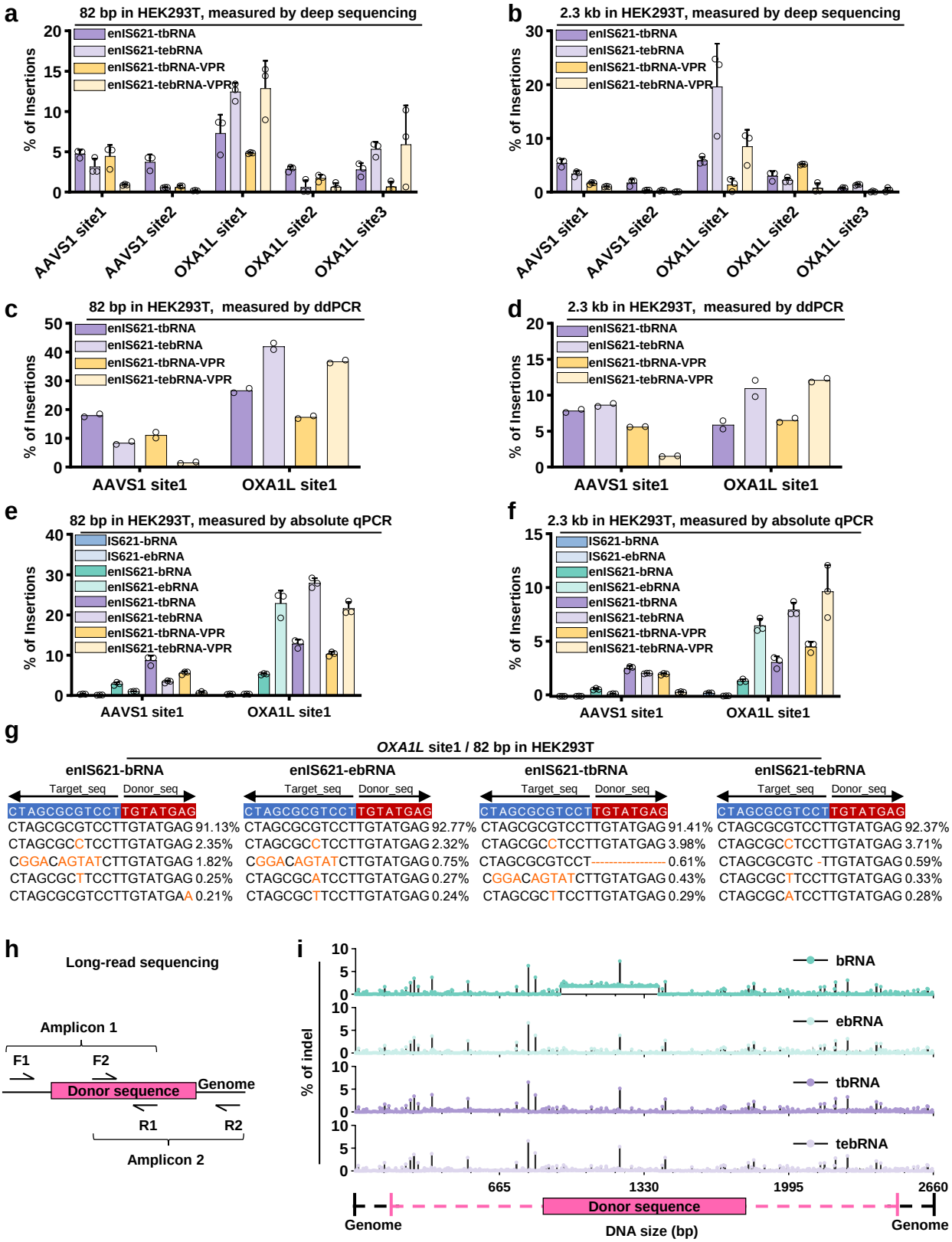
a
82 bp in HEK293T, measured by deep sequencing
% of Insertions
enIS621-tbRNA
enIS621-tebRNA
enIS621-tbRNA-VPR
enIS621-tebRNA-VPR
AAVS1 site1
AAVS1 site2
OXA1L site1
OXA1L site2
OXA1L site3
b
2.3 kb in HEK293T, measured by deep sequencing
c
82 bp in HEK293T, measured by ddPCR
d
2.3 kb in HEK293T, measured by ddPCR
e
82 bp in HEK293T, measured by absolute qPCR
IS621-bRNA
IS621-ebRNA
enIS621-bRNA
enIS621-ebRNA
f
2.3 kb in HEK293T, measured by absolute qPCR
g
OXA1L site1 / 82 bp in HEK293T
enIS621-bRNA
enIS621-ebRNA
enIS621-tbRNA
enIS621-tebRNA
Target_seq
Donor_seq
CTAGCGCGTCCTTGTATGAG
CTAGCGCGTCCTTGTATGAG 91.13%
CTAGCGCGTCCTTGTATGAG 92.77%
CTAGCGCGTCCTTGTATGAG 91.41%
CTAGCGCGTCCTTGTATGAG 92.37%
CTAGCGCCTCCTTGTATGAG 2.35%
CTAGCGCCTCCTTGTATGAG 2.32%
CTAGCGCCTCCTTGTATGAG 3.98%
CTAGCGCCTCCTTGTATGAG 3.71%
CGGACAGTATCTTGTATGAG 1.82%
CGGACAGTATCTTGTATGAG 0.75%
CTAGCGCGTCCT---------- 0.61%
CTAGCGCGTC -TTGTATGAG 0.59%
CTAGCGCTTCCTTGTATGAG 0.25%
CTAGCGCATCCTTGTATGAG 0.27%
CGGACAGTATCTTGTATGAG 0.43%
CTAGCGCTTCCTTGTATGAG 0.33%
CTAGCGCGTCCTTGTATGAA 0.21%
CTAGCGCTTCCTTGTATGAG 0.24%
CTAGCGCTTCCTTGTATGAG 0.29%
CTAGCGCATCCTTGTATGAG 0.28%
h
Long-read sequencing
Amplicon 1
F1
F2
Donor sequence
Genome
R1
R2
Amplicon 2
i
% of indel
bRNA
ebRNA
tbRNA
tebRNA
665
1330
1995
2660
Donor sequence
Genome
Genome
DNA size (bp)

Supplementary Figure 6: Comprehensive evaluation of IS621- and enIS621-mediated insertion efficiency and precision across donor sizes and bRNA formats.

a-f, Insertion efficiency at endogenous loci in HEK293T cells mediated by IS621 or enIS621 recombinases with different bRNA formats, with or without transcriptional activators, assessed by multiple methods. Deep sequencing was used to compare insertion efficiencies for an 82 bp donor (**a**) and a 2.3 kb donor (**b**). ddPCR was used to compare insertion efficiencies for an 82 bp donor (**c**) and a 2.3 kb donor (**d**). Absolute quantitative PCR was used to compare insertion efficiencies for an 82 bp donor (**e**) and a 2.3 kb donor (**f**). **g,** Genotype distribution at the 5′ junction of the insertion site during enIS621-mediated insertion of an 82 bp donor with different bRNA formats. **h,** Schematic illustration of potential structural abnormalities within the integration products and the corresponding PCR amplification strategy. **h**, Schematic of long-read sequencing strategy used to evaluate the integrity of integration products. Two PCR amplicons spanning the donor sequence and flanking genomic regions were generated using primer pairs F1/R1 and F2/R2 to ensure full coverage of the integration locus. **i**, Per-base indel frequency across the integration region determined from long-read sequencing data. Each dot represents the percentage of reads containing an insertion or deletion at the corresponding position. The four panels correspond to different bRNA formats (bRNA, ebRNA, tbRNA, and tebRNA). Data are presented as means ± s.d., ddPCR, $n = 2$; RT-qPCR, $n = 3$; deep sequencing, $n = 3$; long-read sequencing $n = 3$ independent biological replicates.

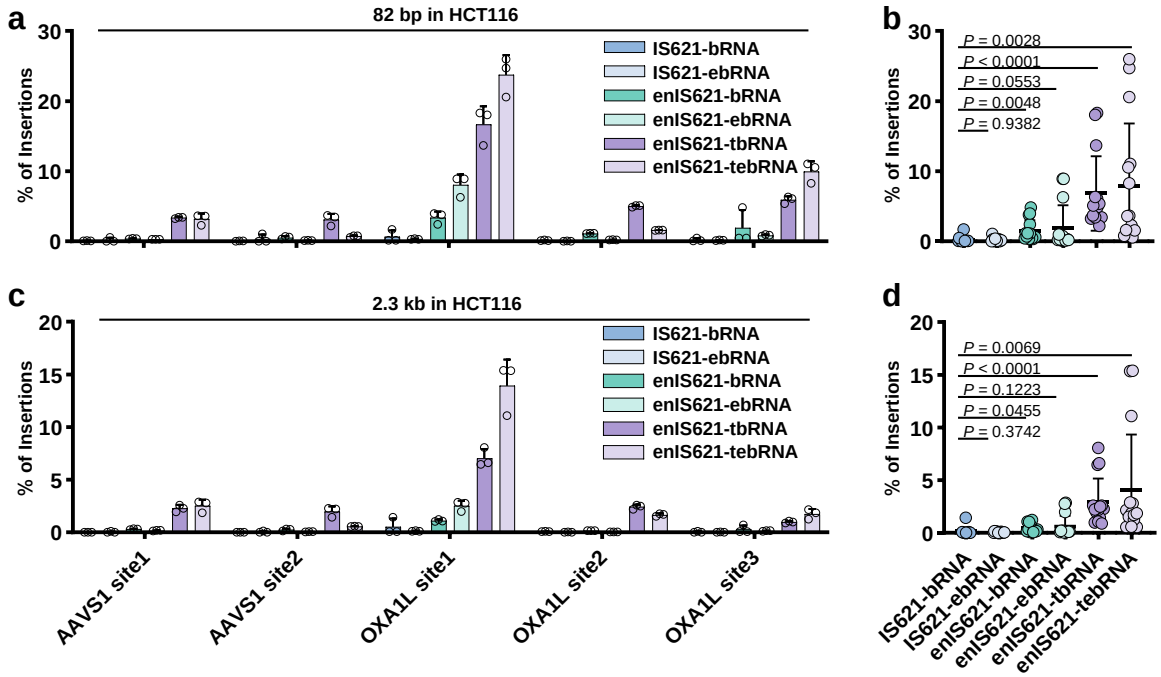
a
82 bp in HCT116
% of Insertions
30
20
10
0
IS621-bRNA
IS621-ebRNA
enIS621-bRNA
enIS621-ebRNA
enIS621-tbRNA
enIS621-tebRNA
b
% of Insertions
P = 0.0028
P < 0.0001
P = 0.0553
P = 0.0048
P = 0.9382
c
2.3 kb in HCT116
% of Insertions
20
15
10
5
0
IS621-bRNA
IS621-ebRNA
enIS621-bRNA
enIS621-ebRNA
enIS621-tbRNA
enIS621-tebRNA
AAVS1 site1
AAVS1 site2
OXA1L site1
OXA1L site2
OXA1L site3
d
% of Insertions
P = 0.0069
P < 0.0001
P = 0.1223
P = 0.0455
P = 0.3742
IS621-bRNA
IS621-ebRNA
enIS621-bRNA
enIS621-ebRNA
enIS621-tbRNA
enIS621-tebRNA

Supplementary Figure 7: enIS621-mediated insertion editing at endogenous loci in HCT116 cells using various bRNA formats.

a-d, Deep sequencing analysis of insertion efficiency for an 82 bp donor or 2.3 kb donor at endogenous loci in HCT116 cells mediated by IS621 or enIS621 recombinases with various bRNA formats. Insertion efficiency comparisons across five endogenous loci (**a,c**) and a summary dot plot of endogenous insertion activities (**d,e**). Data are presented as means ± s.d., $n = 3$ independent biological replicates. *P* values were calculated by Two-tailed unpaired Student's t test.

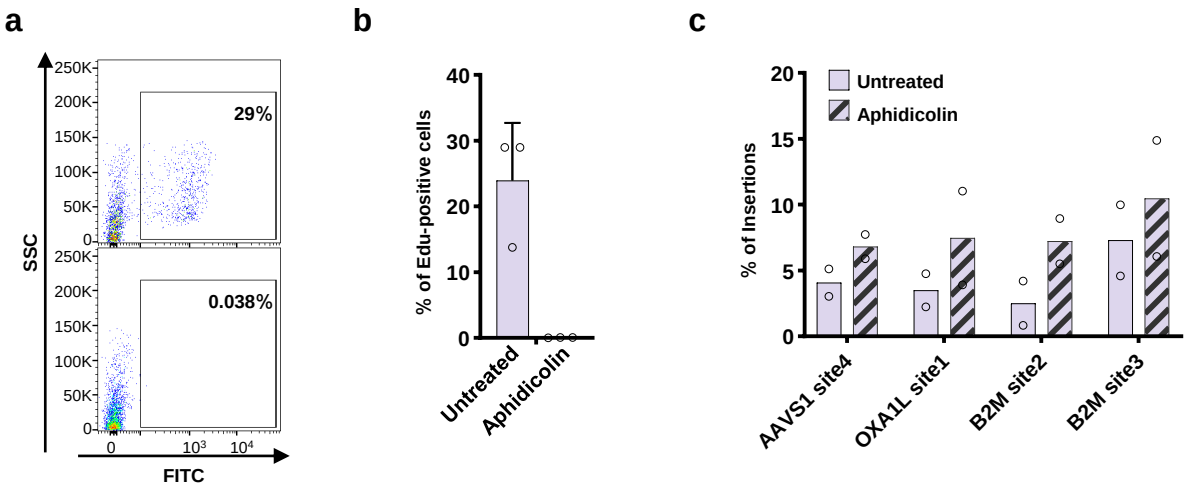
a
b
c
SSC
FITC
29%
0.038%
% of Edu-positive cells
Untreated
Aphidicolin
% of Insertions
AAVS1 site4
OXA1L site1
B2M site2
B2M site3

Supplementary Figure 8: Analysis of cell cycle dependence of enIS621-tebRNA-mediated insertion editing.

a, Assessment of nascent DNA synthesis in RPE-1 cells by EdU incorporation followed by flow cytometry analysis, measured 6 h after aphidicolin treatment. **b,** Quantitative analysis of the proportion of S-phase cells in untreated and aphidicolin-treated conditions. Data are presented as means ± s.d., $n = 3$ independent biological replicates. **c,** ddPCR analysis of insertion editing efficiency mediated by enIS621-tebRNA using a 2.3 kb donor in untreated and aphidicolin-treated RPE-1 cells. Data are presented as means ± s.d., $n = 2$ independent biological replicates.

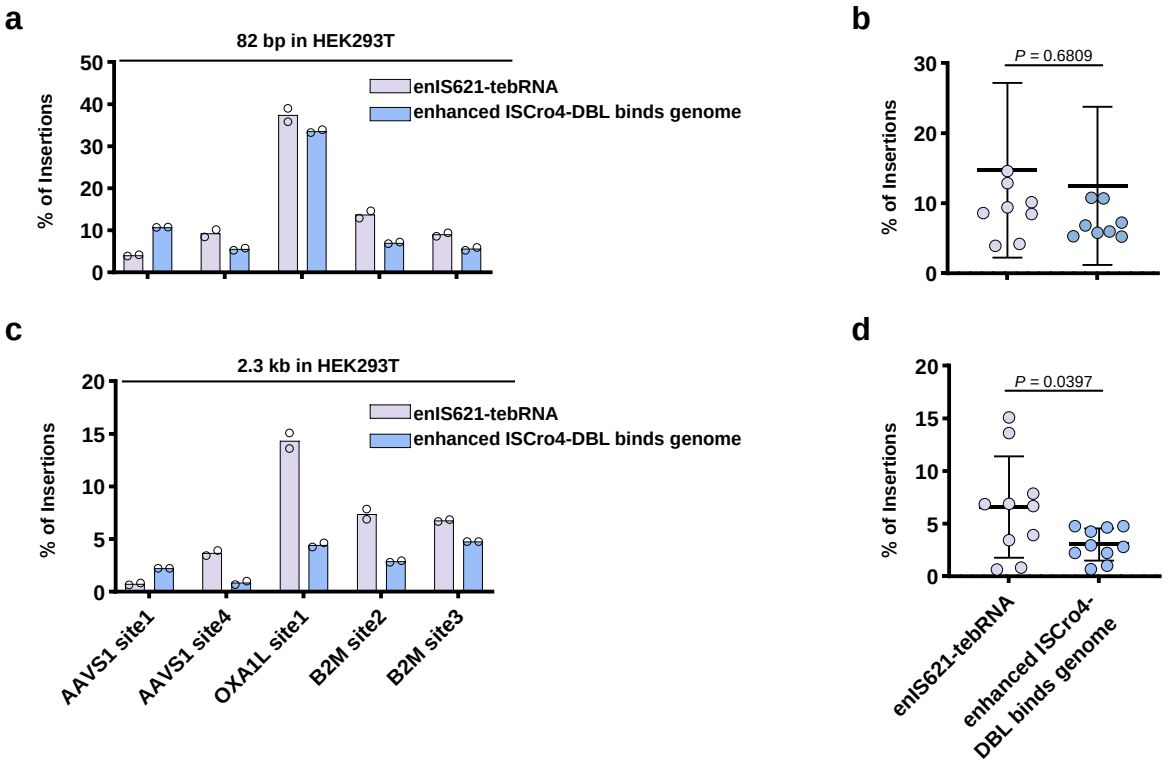
a
82 bp in HEK293T
% of Insertions
50
40
30
20
10
0
enIS621-tebRNA
enhanced ISCro4-DBL binds genome
b
P = 0.6809
% of Insertions
30
20
10
0
c
2.3 kb in HEK293T
% of Insertions
20
15
10
5
0
enIS621-tebRNA
enhanced ISCro4-DBL binds genome
AAVS1 site1
AAVS1 site4
OXA1L site1
B2M site2
B2M site3
d
P = 0.0397
% of Insertions
20
15
10
5
0
enIS621-tebRNA
enhanced ISCro4-DBL binds genome

Supplementary Figure 9: enIS621 and IScro4-mediated insertion editing at endogenous loci in HEK293T cells.

a-d, ddPCR analysis of insertion efficiency for an 82 bp donor or 2.3 kb donor at endogenous loci in HEK293T cells mediated by enIS621 with tebRNA or IScro4 with split bRNA in which DBL targets the genome. Insertion efficiency comparisons across five endogenous loci (**a,c**) and a summary dot plot of endogenous insertion activities (**b,d**). Data are presented as means ± s.d., $n = 2$ independent biological replicates. *P* values were calculated by Two-tailed unpaired Student's t test.

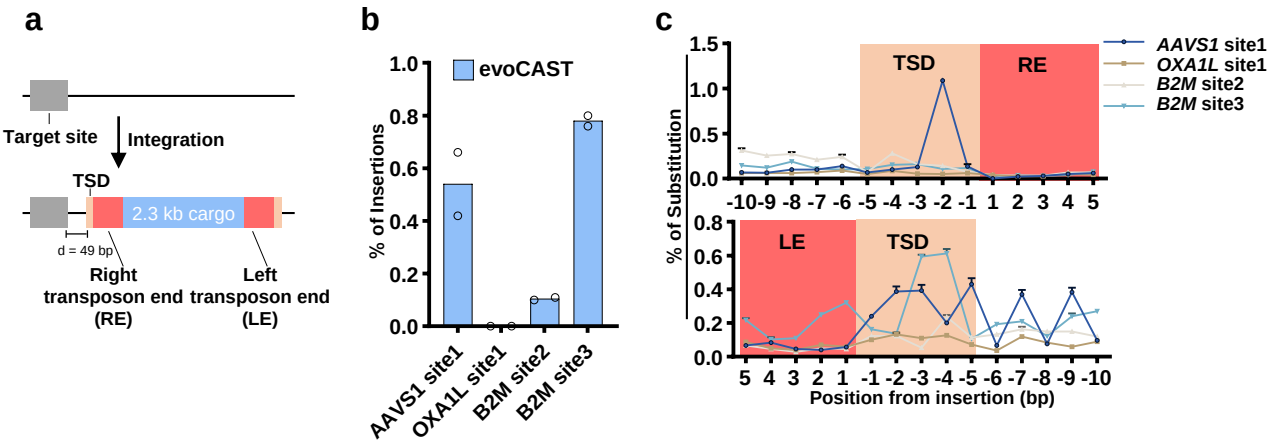
a
Target site
Integration
TSD
2.3 kb cargo
d = 49 bp
Right transposon end (RE)
Left transposon end (LE)
b
evoCAST
% of Insertions
1.0
0.8
0.6
0.4
0.2
0.0
AAVS1 site1
OXA1L site1
B2M site2
B2M site3
c
% of Substitution
1.5
1.0
0.5
0.0
TSD
RE
-10 -9 -8 -7 -6 -5 -4 -3 -2 -1 1 2 3 4 5
LE
TSD
0.8
0.6
0.4
0.2
0.0
5 4 3 2 1 -1 -2 -3 -4 -5 -6 -7 -8 -9 -10
Position from insertion (bp)
AAVS1 site1
OXA1L site1
B2M site2
B2M site3

Supplementary Figure 10: evoCAST-mediated insertion editing at endogenous loci in HEK293T cells.

a, Schematic of evoCAST-mediated endogenous DNA integration. **b,** ddPCR analysis of insertion efficiency for a 2.3 kb donor at four endogenous loci in HEK293T cells mediated by evoCAST. **c,** Quantification of base substitution mutations within a 15-bp window surrounding the genome-transposon right and left junctions for evoCAST insertions across four genomic target sites. Data are presented as means ± s.d., ddPCR, $n = 2$; deep sequencing, $n = 3$ independent biological replicates.

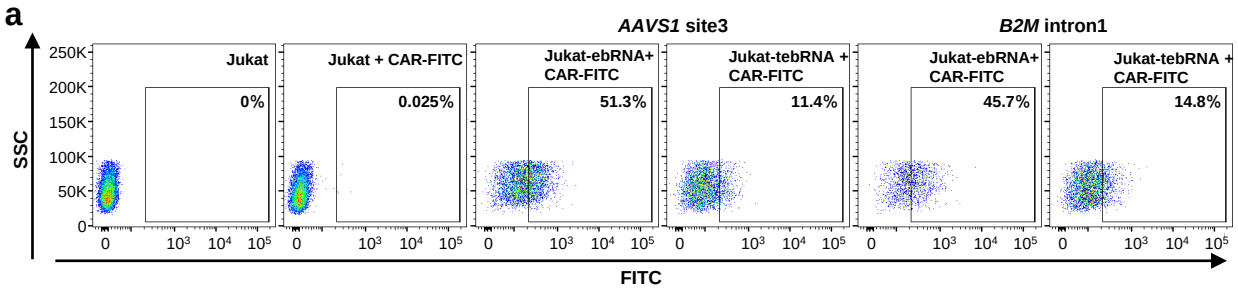

b

enIS621-ebRNA — *B2M* intron1 in HEK293T

5′ junction		3′ junction
98.37%	TGCGCACCCCCTTGTATGAG	TTAACAGTATCTTCCCCACT 98.78%
0.27%	TGCACACCCCCTTGTATGAG	TTCACAGTATCTTCCCCACT 0.13%
0.10%	TGTGCACCCCCTTGTATGAG	TTACCAGTATCTTCCCCACT 0.11%
0.07%	TGCGCACCCCCTTGTATGAA	TTAACAGTATCTTCCCCACC 0.07%
0.06%	TGCGCACCCCCTTGTATNAG	TTAACAGTATCTTCCCCACN 0.05%

enIS621-tebRNA — *B2M* intron1 in HEK293T

5′ junction		3′ junction
98.52%	TGCGCACCCCCTTGTATGAG	TTAACAGTATCTTCCCCACT 98.80%
0.23%	TGCACACCCCCTTGTATGAG	TTCACAGTATCTTCCCCACT 0.10%
0.08%	TGTGCACCCCCTTGTATGAG	TTAACAGTATCTTCCCCACC 0.08%
0.07%	TGCGCACCCC -TTGTATGAG	TTACAGTATCTTCCCCACT 0.08%
0.06%	TGCGCACCCCCTTGTANGAG	TTAACAGTATCTTCCCCACN 0.04%

enIS621-ebRNA — *B2M* intron1 in Jurkat

5′ junction		3′ junction
98.58%	TGCGCACCCCCTTGTATGAG	TTAACAGTATCTTCCCCACT 98.80%
0.23%	TGCACACCCCCTTGTATGAG	TTCACAGTATCTTCCCCACT 0.10%
0.10%	TGTGCACCCCCTTGTATGAG	TTACCAGTATCTTCCCCACT 0.08%
0.06%	TGCGCACCCCCTTGTATGAA	TTAACAGTATCTTCCCCACC 0.07%
0.05%	TGCGCACCCCCTTGTATNAG	TTAACAGTATCTTCCCCACN 0.04%

enIS621-tebRNA — *B2M* intron1 in Jurkat

5′ junction		3′ junction
98.56%	TGCGCACCCCCTTGTATGAG	TTAACAGTATCTTCCCCACT 98.75%
0.24%	TGCACACCCCCTTGTATGAG	TTAACAATATCTTCCCCACT 0.13%
0.08%	TGTGCACCCCCTTGTATGAG	TTCACAGTATCTTCCCCACT 0.10%
0.07%	TGCGCACCCC -TTGTATGAG	TTAACAGTATCTTCCCCACC 0.06%
0.06%	TGCGCACCCCCTTGTATGNG	TTACCAGTATCTTCCCCACT 0.06%

c

enIS621-bRNA — *AAVS1* site1 in HEK293T

5′ junction		3′ junction
98.54%	TTAACCGGCCCTTGTATGAG	TTAACAGTATCTGGGAATAT 98.90%
0.16%	TTAACTGGCCCTTGTATGAG	TTAACAGTATCTGGGAATAG 0.16%
0.14%	TTAACCGGCCCTTGTATGAA	TTAACAGTATCTGGGAAGAT 0.05%
0.08%	TTAACCGACCCTTGTATGAG	TTACCAGTATCTGGGAATAT 0.05%
0.06%	TTAACCGGCCNTTGTATGAG	TTCACAGTATCTGGGAATAT 0.05%

enIS621-tbRNA — *AAVS1* site1 in HEK293T

5′ junction		3′ junction
98.65%	TTAACCGGCCCTTGTATGAG	TTAACAGTATCTGGGAATAT 98.78%
0.14%	TTAACCGGCCCTTGTATGAA	TTAACAGTATCTGGGAATAG 0.13%
0.12%	TTAACTGGCCCTTGTATGAG	TTAACAGTATCGGGGAATAT 0.07%
0.06%	TTAACCGACCCTTGTATGAG	TTAACAGTATTTGGGAATAT 0.05%
0.06%	TTAACCGGCCCTTGTATGAN	TTACCAGTATCTGGGAATAT 0.05%

enIS621-bRNA — *AAVS1* site1 in Huh-7

5′ junction		3′ junction
98.70%	TTAACCGGCCCTTGTATGAG	TTAACAGTATCTGGGAATAT 98.69%
0.14%	TTAACCGGCCCTTGTATGAA	TTAACAGTATCTGGGAATAG 0.14%
0.12%	TTAACCGACCCTTGTATGAG	TTAACAGTATCTTGGAATAT 0.10%
0.11%	TTAACTGGCCCTTGTATGAG	TTAACAGTATCGGGGAATAT 0.09%
0.06%	TTAACCGGCCCTTGTATNAG	TTAACAGTATCTGGGAAGAT 0.06%

enIS621-tbRNA — *AAVS1* site1 in Huh-7

5′ junction		3′ junction
94.41%	TTAACCGGCCCTTGTATGAG	TTAACAGTATCTGGGAATAT 98.76%
4.42%	TTAACTGGCCCTTGTATGAG	TTAACAGTATCTGGGAATAG 0.13%
0.13%	TTAACCGGCCCTTGTATGAA	TTAACAGTATCGGGGAATAT 0.08%
0.06%	TTAACCGGCCCTTGTATGNG	TTAACAGTATTTGGGAATAT 0.05%
0.06%	TTAACCGACCCTTGTATGAG	TTCACAGTATCTGGGAATAT 0.05%

Supplementary Figure 11: Junction genotype analysis and CAR expression following enIS621-mediated insertion in multiple human cell types.
a, CD19 CAR expression in Jurkat cells following insertion of the CD19 CAR sequence mediated by enIS621-ebRNA or enIS621-tebRNA. **b,** Genotype distribution at the 5′ and 3′ junctions of the insertion site in HEK293T and Jurkat cells during enIS621-ebRNA- or enIS621-tebRNA-mediated CD19 CAR insertion. **c,** Genotype distribution at the 5′ and 3′ junctions of the insertion site in HEK293T and Huh-7 cells during enIS621-bRNA or enIS621-tbRNA-mediated Factor IX insertion.